



1 **Determining the susceptibility of soils materials to erosion by rain-**
2 **impacted flows**

3

4 P.I.A. Kinnell

5 Institute for Applied Ecology, University of Canberra, Australia

6 Correspondence to: P.I.A. Kinnell (peter.kinnell@canberra.edu.au)

7

8 **Abstract**

9

10 Conceptually, rain has a capacity to cause erosion (rainfall erosivity) and soils have a susceptibility to
11 erosion by rainfall (soil erodibility) but no absolute measure of rainfall erosivity exists. Consequently,
12 soil erodibility is nothing more than an empirical coefficient in the relationship between an index of
13 rainfall erosivity and soil loss. Erosion by rain-impacted flow is influenced by the size, velocity and
14 impact frequency of the raindrops but also flow depth and velocity. Experiments with artificial rainfall
15 falling on sloping surfaces in the field usually do not enable flow depth and velocity to be well
16 measured or controlled. Also, sprays produce artificial rainfall where the spatial uniformity in rainfall
17 intensity, drop size and frequency is often less than desirable. Artificial rainfall produced by pendant
18 drop formers can produce rainfall that has better spatial uniformity. Equipment for controlling flow
19 depth and velocity over eroding surfaces has been developed and used to calibrate the effect of flow
20 depth on the discharge of sediment by rain-impacted flow using artificial rainfall having a uniform
21 drop-size distribution under laboratory conditions. Once calibrated, laboratory experiments can be
22 conducted to rank soils according to their susceptibility to erosion under the flows impacted by the
23 artificial rainfall under conditions where the erosive stress applied to the eroding surface is well
24 controlled.

25

26 Key Words: Rainfall erosion; soil erodibility; laboratory experiments; rainfall uniformity.

27



28 **1 Introduction**

29

30 Conceptually, rain has a capacity to cause erosion (rainfall erosivity) and soils have a
31 susceptibility to erosion by rainfall (soil erodibility). Rainfall erosion is a complex process and, in
32 reality, no absolute measure of rainfall erosivity exists. Various parameters (eg. rainfall kinetic energy)
33 and combinations of parameters (eg. product of storm rainfall energy and the maximum 30-minute
34 intensity) are used as indices of rainfall erosivity and, as a consequence, soil erodibility is nothing more
35 than an empirical coefficient in the relationship between an index of rainfall erosivity and soil loss. Also
36 the ranking of soils according to their erodibility values can vary depending on how those erodibilities
37 are determined experimentally and the model being used. For example, Kinnell and Risse (1998)
38 presented soil erodibility values in SI units obtained using runoff and soil loss plot data at a number of
39 locations in the USA for the Universal Soil Loss Equation (USLE; Wischmeier and Smith, 1965, 1978),
40 which uses the EI_{30} as the event erosivity index, and the USLE-M which uses the product of the runoff
41 ratio (Q_R) and EI_{30} . Table 1 shows the ranking obtained using the soil erodibilities for the USLE (K)
42 published by Risse et al (1993) and the erodibilities observed Kinnell and Risse for the USLE and the
43 USLE-M (K_{UM}) for the bare fallow plots at 14 locations. All three rankings are different. In addition
44 field experiments designed to determine K factor values using artificial rainfall in the USA measure soil
45 loss under different moisture states (dry, wet, very wet) and weight the result so as to provide an
46 estimate of K for central USA (Romkens, 1985). Consequently, K factor values determined using the
47 soil erodibility nomograph (Wischmeier et al, 1971) need to be adjusted for the difference in climate
48 when applied outside that geographic area (USDA, 2008).

49

50 Modern understanding of rainfall erosion recognizes that rainfall erosion is caused by the
51 expenditure of the kinetic energies of raindrops and surface water flows acting either singly or together.
52 Detachment of soil material from the soil surface is essential before the transport of soil material away
53 from the site of detachment leads to soil erosion. Detachment in sheet and interrill erosion which erode
54 the most chemically active layer of the soil, the soil surface, is dominated by the expenditure of the



55 kinetic energy of the impacting raindrops. Raindrop impact is also involved in transporting soil particles
56 in rain-impacted flows. The WEPP model ((Flanagan and Nearing, 1995) was developed to predict soil
57 loss by modelling flow driven erosion in rills and raindrop driven erosion in interrill areas as separate
58 processes. In the WEPP interrill erosion model, the event erosivity index is the product of the runoff
59 rate (q_w) and rainfall intensity (I) so that D_s (mass/area/time), the rate sediment is discharged from the
60 interrill area, is given by

$$61 \quad D_s = k_i q_w I S_f \quad (1)$$

62 where, k_i is the interrill erodibility and S_f is a function of slope gradient. However, the ranking of the
63 soils in the field experiments of Elliot (1989) depends on whether the plots had inclined surfaces similar
64 to those used in ridge tillage agricultural systems or were relatively flat (Table 2). The correlation
65 between the interrill erodibilities on the flat and ridged plots was also poor (Figure 1). One reason for
66 this is that sediment discharge rate (q_s , mass/width/time) generated by raindrop-induced saltation that
67 often controls erosion on sheet and interrill areas is influenced by a water depth (h), drop size and flow
68 velocity (u),

$$69 \quad q_s(h,d) = k_{sd} u I_d f[h,d] \quad (2)$$

70 where k_{sd} is a coefficient that depends the characteristics of material being eroded, u is flow velocity, I_d
71 is the intensity of the rain made up of drops of size d , and $f[h,d]$ is a function accounting for the effect
72 on sediment discharge of the interaction between flow depth (h) and drop size (Kinnell, 1993b), but the
73 effects of u , I_d , h and d are not taken into account in Eq. (1). Many subsequent experiments have been
74 performed in many parts of the world, in some cases, the surfaces have been inclined at angles
75 commonly observed in ridge tillage systems used in agriculture, but in many cases, relatively flat
76 surfaces have been used. Consequently, given the results presented in Table 2, misleading modelled
77 results may have been produced using interrill erodibilities from many experiments because of the lack
78 of adequate control of the factors that influence soil loss generated by rain-impacted flows in those
79 experiments.

80

81 Rain-impacted flows dominate erosion in sheet and interrill erosion areas. As noted above,
82 these areas are important given that erosion removes soil from the soil surface and usually, the soil



83 surface is the most chemically rich and active part of the soil. Consequently, it is important to determine
84 the susceptibility of soil surfaces to erosion by rain-impacted flows when the factors that influence soil
85 loss generated by rain-impacted flows are known and well controlled. As demonstrated here, this is
86 possible under laboratory conditions.

87

88 **2 Equipment**

89

90 The objective of the equipment described here is to produce the situation where an
91 erodible surface is eroded by rain-impacted flow where flow depth and velocity are controlled in order
92 to control the erosive stress applied by the impacting raindrops to the eroding surface. The apparatus
93 shown in Figure 2 is a modification of the one originally developed by Moss and Green (1983).
94 Basically, the erodible material is contained in a box within a flume with an adjustable weir to facilitate
95 the control of flow depth and velocity. A ripple guard is placed at the downstream end to prevent ripples
96 produced by drop impacts affecting the capacity of the weir to control flow depth and velocity. Inflows
97 are controlled so that, together with adjustments to the height of the weir, flow depths and velocities can
98 be set. A rain bleed is used to bleed water from the flume when rainfall is applied in order to maintain
99 the outflow at the inflow rate. This bleed is of major importance in obtaining flow depth and velocity
100 control when flows are very shallow. In experiments using sand by Moss and Green (1983) and Kinnell
101 (1988, 1993b), the eroding area was 500 mm by 500 mm. In the experiments by Kinnell, flow depth
102 prior to rain was measured by having a removable horizontal bridge above the bed and measuring the
103 distance from the top of the bridge to the eroding surface when there was no flow, and the distance to
104 the water surface when the was flow using a vernier depth gauge with a sharp pointed end. Contact with
105 the water and erodible surfaces was detected electrically. A pressure port located at the bottom end of
106 the sand box enabled the flow depth to be monitored during rain when eroding sand (Kinnell, 1988).

107

108 Often, laboratory experiments on rainfall erosion involve packing loose soil material into boxes
109 and exposing them to rain. Loose soil can packed into the box as an alternative to sand in order to erode



110 soil under controlled flow conditions. However, a version of the apparatus has also been developed that
111 enables experiments to be undertaken using intact soil monoliths having a surface area 250 mm wide by
112 500 mm long (Kinnell and McLachlan, 1989). Experiments have been performed on surface soils from
113 Ginninderra near Canberra, Australia and near Coolabah in New South Wales using this apparatus.
114 Metal sampling frames as depicted in Figure 3 were used to collect blocks of soil 500 mm long, 250
115 mm wide and 100 mm deep. The area to be taken was dug around to produce a block of soil a little
116 bigger than 500 mm by 250 mm by 100 mm deep. The frame was bevelled on the bottom edged to aid
117 cutting the soil as it was pushed down over the block. Once in place, 125 mm by 5.6 mm nails were
118 then hammered through the sides to provide a support structure. The bottom of the block was then cut to
119 free the monolith and the frame tipped gently on its side. The bottom of the monolith was then trimmed
120 square with the base and the monolith tipped back onto a supporting base of marine ply having an area a
121 little larger than 500 mm by 250 mm. A similar piece of wood was placed on the top of the frame and
122 straps used to make a package for transport. Prior to the experiments with rain-impacted flow, the top
123 piece of wood was removed and the frame containing the soil supported by the marine ply base placed
124 in the flume. The monolith was then saturated by wetting from the bottom. Each monolith was
125 subjected to 10 minute of rainfall with $d = 2.7$ mm produced 11.2 m above the surface and a rainfall
126 intensity of 64 mm/h with flow depth at the maximum and $u = 20$ mm/s as a pre-treatment. Then 10
127 mins of rain was applied at each of 4 flow depths with $I_d = 64$ mm/h and $u = 20$ mm/s with flow depths
128 decreasing over the range 7.5 mm to 3.2 mm.

129

130 Some soil particles detached by raindrops impacted flows travel in the flow in suspension while
131 others saltate or roll along the surface. Saltation and rolling can occur in unimpacted flows only if they
132 have flow velocities that exceed certain critical values. Below these critical flow velocities, soil
133 particles may be induced saltate or roll only in association with the impact of individual raindrop
134 impacts. Flow velocities below those causing flow driven saltation and rolling are common in many
135 sheet and interrill erosion areas and consequently, the experiments were undertaken at flow velocities
136 set about 20 mm/s so that only raindrop driven saltation and rolling could occur for particles not
137 travelling in complete suspension.



138

139 Modules producing pendant raindrops from hypodermic needles 11.2 m above the eroding
140 surface produced the artificial rainfall applied in the experiments reported by Moss and Green (1983)
141 and Kinnell (1988, 1993b). The modules produced drops over an area 1 m by 1 m. The needles were
142 spaced 25 mm apart. Rainfall intensity was controlled using a metering pump because previous work
143 established that using hydrostatic pressure as a mechanism to control rainfall intensity did not provide
144 good temporal control of rainfall intensity. The modules were moved back and forth 250 mm along the
145 line of flow at 4.2 mm/s. Spatial variations in rainfall intensity do occur in rain produced from
146 hypodermic needles due to variations in the drop production rate between nearby needles and variations
147 in the trajectory of drop fall. Moving the modules back and forth helps produce high levels of spatial
148 uniformity in rainfall intensity which are important in facilitating the movement of particles travelling
149 by raindrop induced saltation and rolling (Kinnell, 1991). In raindrop induced saltation and rolling
150 particles move a limited distance from the point of drop impact and remain sitting on top of the soil
151 matrix until disturbed again by a subsequent drop impact. Consequently, any positive or negative
152 variation from the mean in respect to drop size, drop velocity and drop impact frequency at the
153 downstream end of an eroding surface will result in sediment discharges that differ from those where
154 these factors are completely uniform spatially.

155

156 **3 Calibration**

157

158 In order to determine soil erodibilities using the apparatus described above, equations that
159 describe the flow depth – drop size function in Eq. (1) specifically for the experimental conditions are
160 needed particularly when, as is often the case in many laboratory situations, drops are travelling at
161 considerably less than terminal velocity. The procedure for setting flow depth involves setting a height
162 for the weir and running a set of inflow rates and measuring the flow depths associated with them.
163 Given data on flow depth and inflow rate, flow velocity is then calculated and the inflow rate meeting
164 the desired flow criteria selected for the erosion experiments.

165



166 Prior to undertaking the experiments to calibrate flow depth and velocity, the erodible surface
 167 should have been prepared and put in place. Experiments for determining $f[h,d]$ for drops travelling at
 168 or near terminal velocity by Kinnell (1991, 1993b) were undertaken using beds of 0.2 mm sand, leveled
 169 and smoothed prior to flow conditions being set. 0.2 mm sand was also used for the experiments at
 170 subterminal velocity (Kinnell, 2005a). Beds of uniform sized sand are best to use since all particles have
 171 the same potential rate of travel. The duration of exposure to rain was arbitrarily set at 10 minutes and
 172 gave measureable quantities of eroded material without a loss of material sufficient to change the height
 173 of the surface appreciably from the original height over the bottom half of the eroding surface. Although
 174 0.2 mm was used here in the calibration exercise, Eq. 2 has been shown to apply to the erosion of beds
 175 of sand containing particles ranging in size between 0.1 mm and 0.9 mm (Kinnell 1991, 1993b).

176

177 The experiments undertaken by Kinnell (1991, 1993b) showed that the rate sand was discharged
 178 varied linearly with rainfall intensity and flow velocity as indicated in Eq.(2). Sediment discharge (q_s ,
 179 mass/width/time) is given by the product of water discharge (q_w , volume/width/time) and sediment
 180 concentration (c_s), the mass of material discharged with the flow per unit volume of water;

181

$$182 \quad q_s = q_w c_s \quad (3)$$

183

184 so that

185

$$186 \quad c_s = q_s / q_w \quad (4)$$

187

188 and, from Eq. (1),

189

$$190 \quad c_{sd} = k_{sd} I_d f[h,d]/h \quad (5).$$

191

192 where c_{sd} is the sediment concentration produced by the impact of drops of size d and k_{sd} is a coefficient
 193 related to the susceptibility of the eroding material to erosion. Dividing both sides of Eq. (5) by I_d gives



194

$$195 \quad c_{sd}/I_d = k_{sd} f[h,d]/h \quad (6),$$

196

197 Consequently, for an eroding surface of uniform sized sand, using sediment concentration per unit
198 rainfall intensity as the dependent variable provides an equation where the effect of the drop size - flow
199 depth interaction can be evaluated even when rainfall intensity and flow velocity vary. Figure 4 shows
200 the relationship between sediment concentration per unit rainfall intensity and flow depth obtained for
201 2.7 mm drop impacting flows at close to terminal velocity over beds of 0.2 mm sand in experiments
202 reported by Kinnell (1991, 1993b). As illustrated by Figure 5, the relationship between sediment
203 concentration per unit rainfall intensity and flow depth determined for 0.2 mm sand provides a
204 mathematical expression that is linearly related to sediment concentration per unit rainfall intensity for
205 sediment discharged from other sand surfaces and this leads to the equation

206

$$207 \quad c_{sd}/I_d = k_s (0.0015 h^2 - 0.0291 h + 0.1443) \quad , d=2.7, h<9 \text{ mm} \quad (7)$$

208

209 where k_s varies with the particle size. In addition, Kinnell and McLachlan (1989) showed that the form
210 of the relationship between sediment concentration and flow depth when rain-impacted flows erode
211 cohesive soil surfaces was the same as that for sand. However, as indicated by Figure 6, a different
212 calibration equation is required when drop size and velocity conditions vary from those used in the
213 experiments that produced Eq. (7).

214

215



216 **4 Ranking surface susceptibility to erosion by rain-impacted flow.**

217

218 In Eq. (7), k_s for 0.2 mm sand is, in theory, equal to 1.0 so that the k_s values for other sized sands
219 are scaled relative to the susceptibility of 0.2 mm sand to erosion by flows impacted by 2.7 mm drops
220 travelling at near terminal velocity. A more general equation for the effect of drop size and eroding
221 material on the ratio of c_{sd} to I_d is given by

222

$$223 \quad c_{sd}/I_d = k_{sd} (a_d h^2 - b_d h + 1.0) \quad (8)$$

224

225 where k_{sd} acts as an index of the susceptibility of the eroding surface to erosion by drops of size d , and
226 a_d and b_d are coefficients that vary with d . For 2.7 mm drops travelling at near terminal velocity and $h <$
227 9mm, $a_d = 0.0104$ and $b_d = 2.017$. Figure 7 shows the application of Eq. (8) when surfaces of soil
228 monoliths were exposed flows impacted by 2.7 mm raindrops travelling at near terminal velocity in the
229 modified version of the apparatus shown in Figure 1. As noted above, the Ginninderra soil monolith
230 came from bare fallow runoff and soil loss plots near Canberra, Australian Capital Territory (Kinnell,
231 1983) while the Oakvale monoliths came from a location near Coolabah, New South Wales, Australia
232 and had differing levels of cryptogamic crust cover. k_{sd} in Eq. (8) is an index of the susceptibility of the
233 soil to erosion only in a qualitative sense.

234

235 In the experiments performed with sand, new surfaces were prepared for each rainfall event. In
236 the experiments with soil monoliths, each monolith was eroded by 4 rainfall events starting with 2
237 rainfall events at the maximum flow depth used. The first event was a pre-treatment but in reality, each
238 rainfall event that precedes another is a pre-treatment to subsequent events. Starting the sequence from
239 the shallowest flow produces a different result (Kinnell et al., 1996).

240

241 Over a limited range of flow depths, a linear relationship also exists with the inverse of flow
242 depth minus 0.1 when the 2.7 mm drops fall from 11.2 m (Figure 8);



243

$$244 \quad c_{sd}/I_d = k_{1sd} / (1/h - 0.1) \quad , d=2.7, 3d < h < 4\text{mm} \quad (9)$$

245

246 where k_{1sd} is a coefficient that is related to the susceptibility of the soil to erosion by rain impacted flow.

247 The upper depth limit is, in the case of drops travelling at close the terminal velocity, equal to $3d$

248 because the cavity carved in the water by the impacting drop had a maximum depth equal to $3d$ (Engel,

249 1966). For flow depths less than about 4 mm ($1/h = 0.25$), the depth of flow imposes an appreciably

250 constraint on particle travel distance so that sediment concentrations divided by $1/h - 0.1$ are less than

251 predicted using the relationship for deeper flows .

252

253 Figure 9 shows the relationships between the sediment concentrations per unit rainfall intensity
254 for the soil monoliths and $1/h - 0.1$. The relative rankings for the susceptibility of the surfaces to
255 erosion using $1/h - 0.1$ and $0.0104 h^2 - 0.2017 h + 1.0$ are similar (Table 3). Equation 9 was also used to
256 determine the erodibility of microphyte-dominated calcareous soils in woodland near Wentworth, New
257 South Wales, Australia (Eldridge and Kinnell, 1997).

258

259 **5 Discussion**

260

261 The method described above is unique to the extent that no other method reported in the
262 literature provides as high a degree of control on the factors known to influence the erosive stress
263 applied to the soil surface when raindrops impact shallow surface water flows. In using the method, the
264 ranking of soils in respect to their susceptibility to erosion is obtained through an empirical factor that
265 results from experiments when flow depth is varied in a manner that controls the erosive stress applied
266 to the soil surface that is not achieved by laboratory and field experiments where natural or artificial
267 rain is applied to inclined surfaces. It can be argued that flow depth is, for a given rainfall, a soil specific
268 property (determined by infiltration, crust formation etc.), so that controlling runoff depth is not



269 required to estimate an erodibility coefficient commonly used in erosion models. However, as illustrated
270 by the erodibility data for WEPP shown in Table 2, that argument is hardly compelling.

271

272 The apparatus shown in Figure 2 can be used under artificial rainfall produced by sprays
273 provided that the depth effect is determined for that rainfall producing system. Spray rainfall simulators
274 are widely used because that have a wide drop size distribution that may be similar to those found in
275 rainfall but many different types of nozzle have been used without good knowledge of the variation of
276 the intensity and kinetic energy of the rain within the target area. As demonstrated by Iserloh et al
277 (2013) and Lassuet al (2014), the drop size, drop velocity and drop impact frequency characteristics of
278 rain produced by many rainfall simulators using nozzles are far from spatially uniform. Also, spatial
279 variations in rainfall characteristics can vary with the pressure of the water supplied to the nozzle and,
280 in many cases, the control of that pressure in not well maintained. As noted earlier, spatial variations in
281 rainfall characteristics particularly in the zone near the bottom end of the eroding surface can have an
282 appreciable influence of sediment discharge under rain-impacted flows. The spatial uniformity of the
283 rainfall characteristics, and control of raindrop size and energy, is better maintained in systems the
284 produce rain from drop formers such as described above.

285

286 Although the method is based on the model described by Eq. 2, the results from the experiments
287 reported above have been used in a qualitative assessment of the susceptibility of the eroding surfaces
288 rather than as quantitative values of erodibility that can be applied to predicting sheet and interrill
289 erosion even though equations that model the effect of flow depth on $f[h,d]$ over the range of drop sizes
290 commonly observed in natural rainfall exists (Kinnell, 1993b). For a surface of uniform sized sand, the
291 particle size distribution of the eroding surface remains constant with time so that k_{sd} remains constant
292 with time. However, as noted above, some soil particles detached by raindrops impacted flows travel in
293 the flow in suspension while others saltate or roll along the surface and as a consequence, particles of
294 different size travel at different rates from the point where there were initially mobilized. This, in effect,
295 results in fast moving particles being winnowed from the eroding surface so that the particle size
296 composition of the particles sitting on the surface changes with time. Also, loose particles sitting on the



297 surface provide a degree of protection against detachment of soil particles from cohesive soil surfaces
298 (Kinnell 2005b, 2006) with the result that k_{sd} varies with time. As noted above, for each soil surface, 10
299 mins of rain was applied to at each of 4 flow depths with $I_d = 64$ mm/h and $u = 20$ mm/s with flow
300 depths decreasing over the range 7.5 mm to 3.2 mm. Using the reverse sequence with flow depth
301 increasing over the range 3.2 to 7.5 mm resulted in a different value of c_{sd}/I_d being obtained being
302 produced for a given flow depth (Kinnell et al, 1996) as a result of the temporal changes that occur on
303 the eroding soil surface. Varying the time of exposure to rain and the length of the eroding surface may
304 also result in different values of c_{sd}/I_d being produced for a given flow. Erosion by rain-impacted flows
305 involves complex interactions between raindrops, flowing water and the soil surface so that the
306 susceptibility of the soil surface to erosion by rain-impacted flow varies in time and space even when
307 rain and flow characteristics do not.

308

309 Although the method described above can be used to provide a qualitative rather than
310 quantitative assessment of the susceptibility of the eroding surfaces to erosion by rain- impacted flows,
311 the high degree of control of the factors that affect the erosive stress provides an environment with a
312 potential to be used in the study of how factors like cohesion affect soil erodibility. It also has the
313 potential to be used in studies on how surfaces eroding by rain-impacted flows mobilize carbon and
314 chemical pollutants to flows that transport them across the landscape.

315

316 **6 Concluding remarks**

317

318 Given flow depth, flow velocity, raindrop size, raindrop velocity and raindrop impact frequency
319 influence the erosive nature of rain-impacted flows, it is necessary to control and measure these factors
320 when determining the susceptibility of soil to erosion by rain-impacted flow. The apparatus shown in
321 Figure 2 is designed to produce controlled and measurable flow conditions over the eroding surface.
322 Such conditions are not achievable when applying artificial rainfall on field plots. While sprays from
323 nozzles may produce drop-size distributions comparable to those that occur in natural rainfall, uniform



324 spatial distributions of rainfall intensity, drop sizes and velocities are seldom achieved. Producing drops
325 from pendent drop formers can produce rainfall that is more spatially uniform provided care is taken to
326 ensure that spatial variations produced by the fact that adjacent droppers do not necessarily produce
327 drops at the same rate are dealt with appropriately.

328

329 In most practical situations, drops produced from pendant drop formers do not achieve terminal
330 velocity before impacting flows over erodible surfaces. Consequently, a calibration equation for the
331 effect of flow depth needs to be obtained that differs from that shown in Figure 4 in many practical
332 cases. Once that calibration equation has been developed, it can, as illustrated in Figure 7 and Table 3,
333 be used obtain qualitative values of the susceptibility of the soil surfaces to erosion by rain-impacted
334 flow.

335

336 In the experiments with soil monoliths reported above, the event duration was arbitrarily set at
337 10 minutes and using a different event duration may produce different results given that exposure to
338 erosion by rain-impacted flow may cause appreciable changes to occur in the soil surface, particularly if
339 the surface has been recently disturbed. In addition to the development of surface crusts which can
340 cause changes in erodibility to occur during a rainfall event, particles travelling by raindrop-induced
341 saltation and rolling may provide a degree of protection against detachment by raindrop impact (Kinnell
342 2005b, 2006) and influence how the particle size characteristics of sediment discharged by rain-
343 impacted flow varies over time (Kinnell, 2009). These factors need to be considered when interpreting
344 results for experiments involving rain-impacted flows. Also, monitoring both sediment discharge and
345 composition may facilitate studies on the effects of factors such as soil chemistry and aggregate stability
346 on erosion by rain-impacted flows.

347



348 **7 References**

349

350 Eldridge, D.J, and Kinnell, P.I.A. 1997. Assessment of erosion rates from microphyte-dominated
351 calcareous soils under rain-impacted flow. *Australian Journal of Soil Research* 35, 475-490.

352 Elliot, W.J, Liebenow, A.M., Laflen, J.M, and Kohl, K.D. 1989. A compendium of soil erodibility data
353 from WEPP cropland soil field erodibility experiments 1987 & 88. NSERL Report No 3, The Ohio
354 State University and the USDA Agricultural Research Service.

355 Engel, O.G. 1966. Crater depths in fluid impacts. *Journal of Applied Physics* 34, 1798-1808.

356 Flanagan, D.C. and Nearing, M.A. 1995 USDA Water Erosion Prediction Project : Hillslope Profile and
357 Watershed Model Documentation, NSERL Report No. 10 USDA- ARS National Soil Erosion
358 Research Laboratory.

359 Iserloh, T., Ries, J.B., Arnáez, J., Boix-Fayos, C., Butzen, V., Cerdà, A., Echeverría, M.T., Fernández-
360 Gálvez, J., Fister, W., Geißler, C., 2013. European small portable rainfall simulators: A comparison
361 of rainfall characteristics. *Catena* 110, 100–112.

362 Kinnell,P.I.A. 1983.The effect of kinetic energy of excess rainfall on soil loss from non-vegetated plots.
363 *Aust. J. Soil Res.* 21, 445-453

364 Kinnell,P.I.A. 1988. The influence of flow discharge on sediment concentrations in raindrop induced
365 flow transport. *Aust. J. Soil Res* 26, 575-582.

366 Kinnell, P.I.A. 1991. The effect of flow depth on erosion by raindrops impacting shallow flow.
367 *Transactions of the American Society of Agricultural Engineers* 34, 161-168.

368 Kinnell, P.I.A. 1993a. Interrill erodibilities based on the rainfall intensity-flow discharge erosivity
369 factor. *Australian Journal of Soil Research* 31, 319-322.

370 Kinnell, P.I.A. 1993b. Sediment concentrations resulting from flow depth – drop size interactions in
371 shallow overland flow. *Transactions of the American Society of Agricultural Engineers* 36, 1099-
372 1103.

373 Kinnell, P.I.A. 2005a. Sediment transport by medium to large drops impacting flows at subterminal
374 velocity. *Soil Science Society of America Journal* 69, 902-905



- 375 Kinnell, P.I.A. 2005b. Raindrop-impact-induced erosion processes and prediction: A review.
376 Hydrological Processes 19, 2815-2844
- 377 Kinnell, P.I.A. 2006. Simulations demonstrating interaction between coarse and fine sediment loads in
378 rain-impacted flow. Earth Surface Processes and landforms 31, 355-367.
- 379 Kinnell, P.I.A. 2009. The influence of raindrop induced saltation on particle size distributions in
380 sediment discharged by rain-impacted flow on planar surfaces. Catena 78, 2-11.
- 381 Kinnell, P.I.A, and McLachlan, C. 1989. Shallow soil monoliths for laboratory studies on soil erosion
382 from undisturbed surfaces. Australian Journal of Soil Research 27, 227-233.
- 383 Kinnell, P.I.A., Ramos, M.C., and Asun Uson. 1996. Method induced variations in erodibility in erosion
384 experiments with rain-impacted flow. Australian Journal of Soil Research 34, 715-720
- 385 Kinnell, P.I.A., and L.M. Risse 1998. USLE-M: Empirical modelling rainfall erosion through runoff
386 and sediment concentration Soil Science Society of America Journal 62, 1667-1672
- 387 Lassu, T., Seeger, M., Peters, P., Keesstra, S., 2014. The Wageningen Rainfall Simulator: Set-up and
388 Calibration of an Indoor Nozzle-Type Rainfall Simulator for Soil Erosion Studies. Land
389 Degradation & Development (Early View). doi:10.1002/ldr.2360
- 390 Moss, A.J., and P Green. 1983. Movement of solids in air and water by raindrop impact. Effects of
391 drop-size and water-depth variations. Australian Journal of Soil Research 21, 257-269.
- 392 Risse, L.M, Nearing, M.A, Nicks, A.D., Laflen, J.M. 1993. Error assessment in the Universal Soil Loss
393 Equation. Soil Science Society of America Journal 57, 825-833.
- 394 Römken, M. J. M. 1985. The soil erodibility factor: A perspective. In Soil Erosion and Conservation,
395 445-461. S. A. El-Swaify, W. C. Moldenhauer, and A. Lo, eds. Ankeny, Iowa: Soil and Water
396 Conservation Society of America.
- 397 USDA. 2008. Draft Science Documentation: Revised Universal Soil Loss Equation Version 2
398 (RUSLE2) USDA-Agricultural Research Service, Washington, D.C.
399 <<http://www.ars.usda.gov/Research/docs.htm?docid=6028>>.
- 400 Wischmeier, W.C, Johnson, C.B. and Cross, B.V. 1971. Soil erodibility nomograph for farmland and
401 construction sites. Journal of Soil and Water Conservation 26, 189-193.



- 402 Wischmeier, W.C., and Smith, D.D. 1965. Predicting rainfall-erosion losses from cropland east of the
403 Rocky Mountains. Agricultural Handbook No. 282. US Dept Agric., Washington, DC.
- 404 Wischmeier, W.C., and Smith, D.D. 1978. Predicting rainfall erosion losses – a guide to conservation
405 planning. Agricultural Handbook No. 537. US Dept Agric., Washington, DC
- 406 .
- 407



Table 1. Soil erodibilities in SI units associated with the USLE published by Risse et al (1993) and the values observed by Kinnell and Risse (1998) for the USLE and USLE-M models

Rank	Erodibility (t hr MJ ⁻¹ mm ⁻¹)										erodibility relative to that at Arnot		
	location	pub K	location	obs K	location	obs K	location	K _{UM}	location	pub k	obs K	K _{UM}	
1	Arnot	0.0026	Arnot	0.0031	Arnot	0.0088	Arnot	0.0088	Arnot	1.0	1.0	1.0	
2	Tifton	0.0066	Tifton	0.0067	Tifton	0.0185	Tifton	0.0185	Tifton	2.5	2.2	2.1	
3	Watkinsville	0.0237	Guthrie	0.0119	Guthrie	0.0256	Watkinsville	0.0256	Watkinsville	9.0	8.5	6.2	
4	Madison	0.0290	Presque Isle	0.0162	Statesville	0.0504	Madison	0.0504	Madison	11.0	17.9	11.8	
5	Guthrie	0.0290	Castana	0.0262	Presque Isle	0.0536	Guthrie	0.0536	Guthrie	11.0	3.8	2.9	
6	Presque Isle	0.0303	Watkinsville	0.0264	Watkinsville	0.0547	Presque Isle	0.0547	Presque Isle	11.5	5.2	6.1	
7	Marcellus	0.0369	Statesville	0.0270	McCredie	0.0728	Marcellus	0.0728	Marcellus	14.0	12.6	9.5	
8	Morris	0.0369	McCredie	0.0327	Castana	0.0737	Morris	0.0737	Morris	14.0	11.1	15.2	
9	Castana	0.0435	Morris	0.0345	Marcellus	0.0836	Castana	0.0836	Castana	16.5	8.5	8.4	
10	Statesville	0.0474	Marcellus	0.0390	Holly Springs	0.0933	Statesville	0.0933	Statesville	18.0	8.7	5.7	
11	La Crosse	0.0500	La Crosse	0.0521	La Crosse	0.0996	La Crosse	0.0996	La Crosse	19.0	16.8	11.3	
12	Holly Springs	0.0672	Madison	0.0554	Madison	0.1037	Holly Springs	0.1037	Holly Springs	25.5	21.5	10.6	
13	McCredie	0.0817	Bathnay	0.0619	Bathnay	0.1228	Bathnay	0.1228	McCredie	31.0	11.1	8.3	
14	Bathnay	0.1027	Holly Springs	0.0667	Morris	0.1337	Bathnay	0.1337	Bathnay	39.0	20.0	14.0	



Table 2 WEPP Interrill erodibilities for flat and ridged plots determined by Kinnell (1993b) from the data presented by Elliot et al (1989).

rank	Interrill erodibility ($10^{-6} \text{ kg s m}^{-4}$)				K_i relative to Heiden	
	Location	Ki.ridge	Location	Ki.flat	Ki.ridge	Ki.flat
1	Heiden	1.62	Portneuf	1.79	1.00	0.53
2	Portneuf	2.31	Sverdrup	2.00	1.43	0.59
3	Sharpsberg	2.51	Barnes-ND	2.02	1.55	0.60
4	Barnes-MN	2.58	Pierre	2.72	1.59	0.81
5	Pierre	2.72	Barnes-MN	2.84	1.68	0.84
6	Barnes-ND	3.06	Woodward	3.04	1.89	0.90
7	Los Banos	3.27	Whitney	3.10	2.02	0.92
8	Williams	3.55	Academy	3.32	2.19	0.99
9	Zahl	3.84	Heiden	3.37	2.37	1.00
10	Academy	3.97	Keith	3.82	2.45	1.13
11	Sverdrup	3.97	Hersh	3.89	2.45	1.15
12	Keith	4.26	Los Banos	4.13	2.63	1.23
13	Whitney	4.38	Zahl	4.19	2.70	1.24
14	Nansene	4.93	Sharpsberg	4.53	3.04	1.34
15	Palouse	5.20	Nansene	4.64	3.21	1.38
16	Amarillo	6.19	Williams	5.10	3.82	1.51
17	Hersh	6.80	Amarillo	5.51	4.20	1.64
18	Woodward	7.56	Palouse	6.41	4.67	1.90

Table 3. Relative susceptibility to erosion by 2.7 mm raindrops travelling at near terminal velocity impacting flows over soil monoliths in the apparatus shown in Figure 1

Soil	relative susceptibility	
	Eq. (10)	Eq.(11)
Ginninderra	1.000	1.000
Oakvale D	0.719	0.700
Oakvale IC	0.345	0.351
Oakvale OC	0.077	0.081

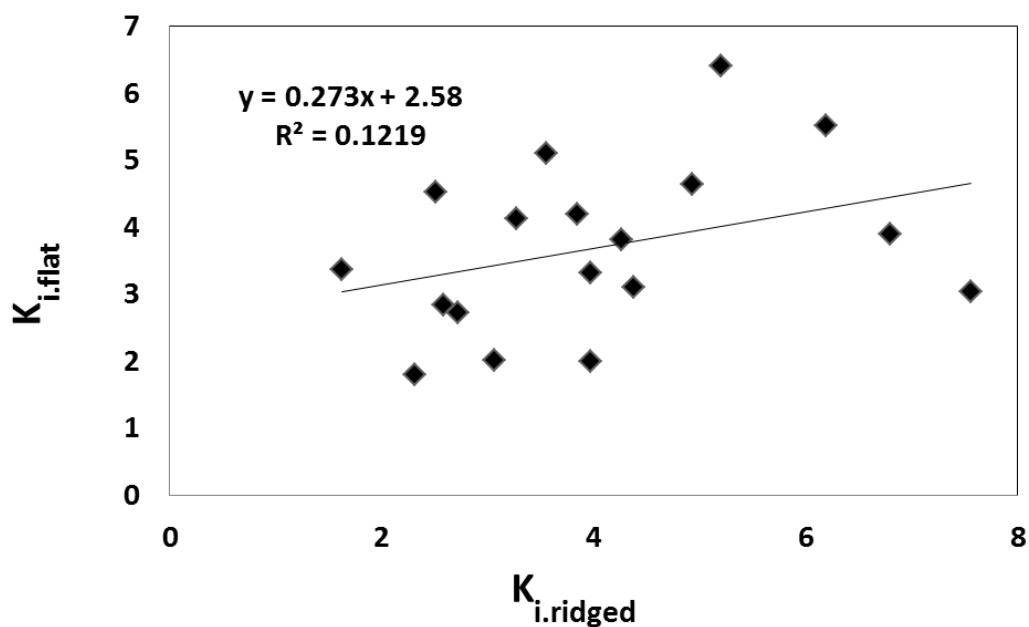


Figure 1. Relationship between flat and ridged erodibilities obtained by Kinnell (1993a) from the experiments of Elliot et al (1989).

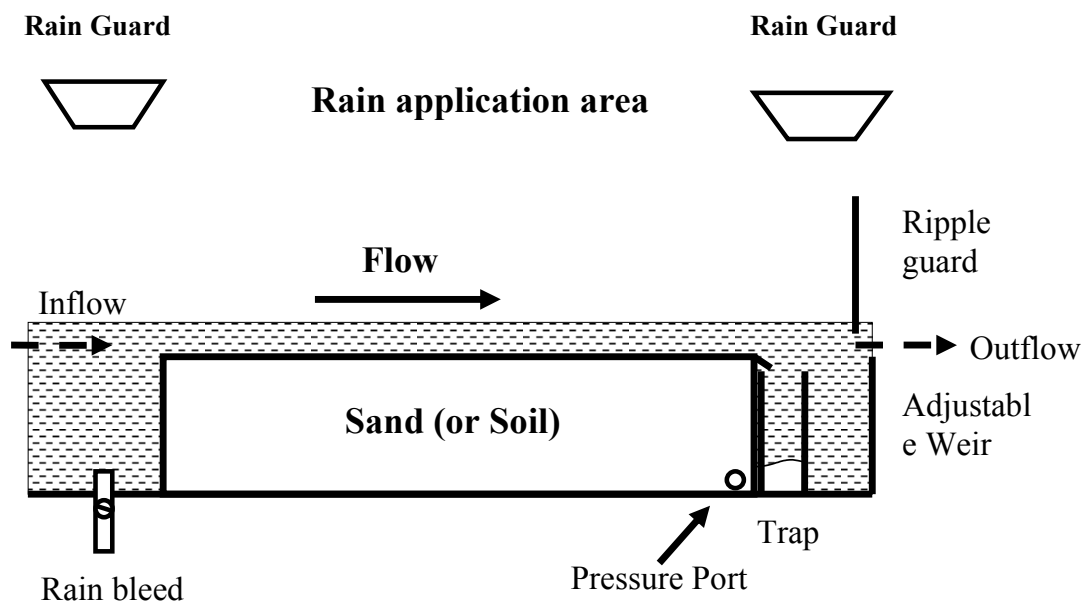


Figure 2. Apparatus used to determine the flow depth function for flows impacted by drops travelling at or near terminal velocity by Kinnell (1993b).

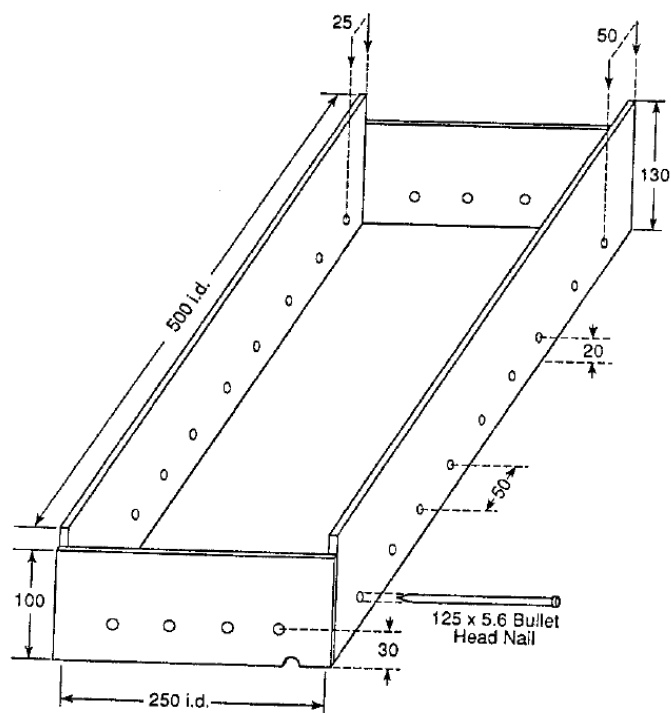


Figure 3. Sampling frame for collecting soil monoliths

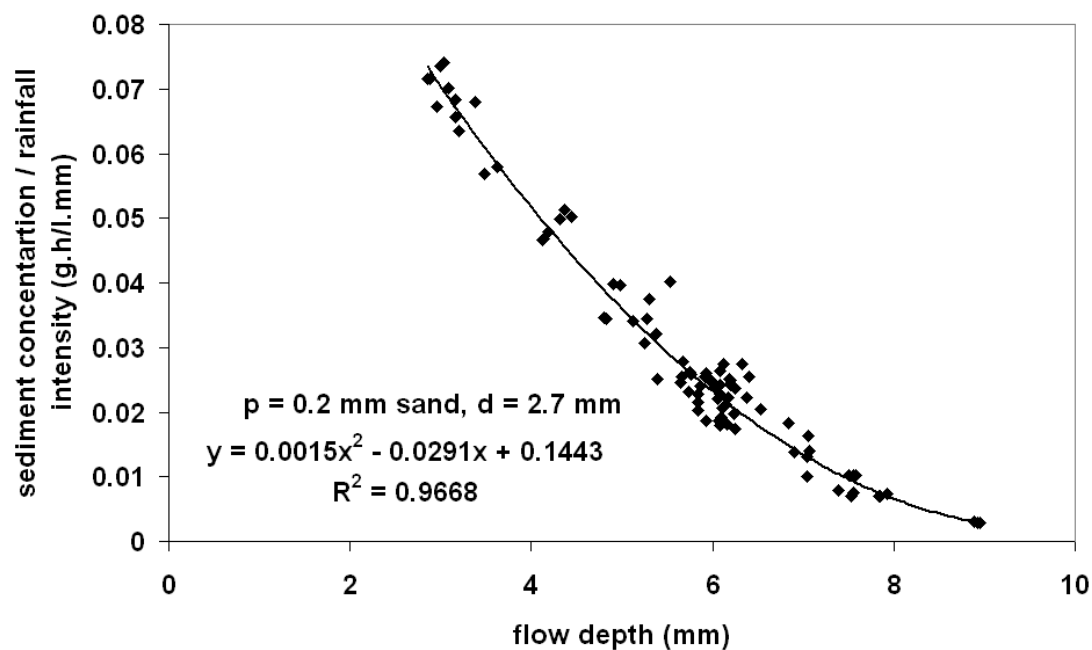


Figure 4. Relationship between sediment concentration per unit rainfall intensity and flow depth for 0.2 mm sand under flows impacted by 2.7 mm drops travelling at close to terminal velocity in experiments reported by Kinnell (1991, 1993b). (From Kinnell, 2009). Note the equation is not valid when $h > 9$ mm.

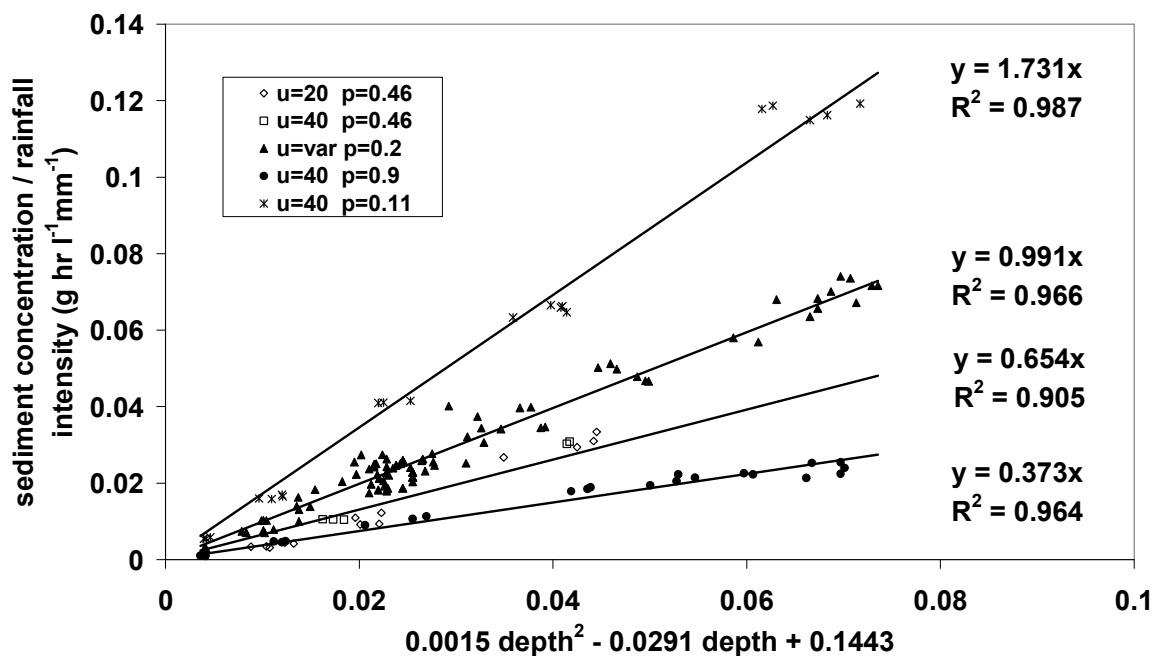


Figure 5. Relationships produced by Eq. (7) for beds of sand of various sizes eroding under flows impacted by 2.7 mm drops travelling at close to terminal velocity (from Kinnell, 2009).

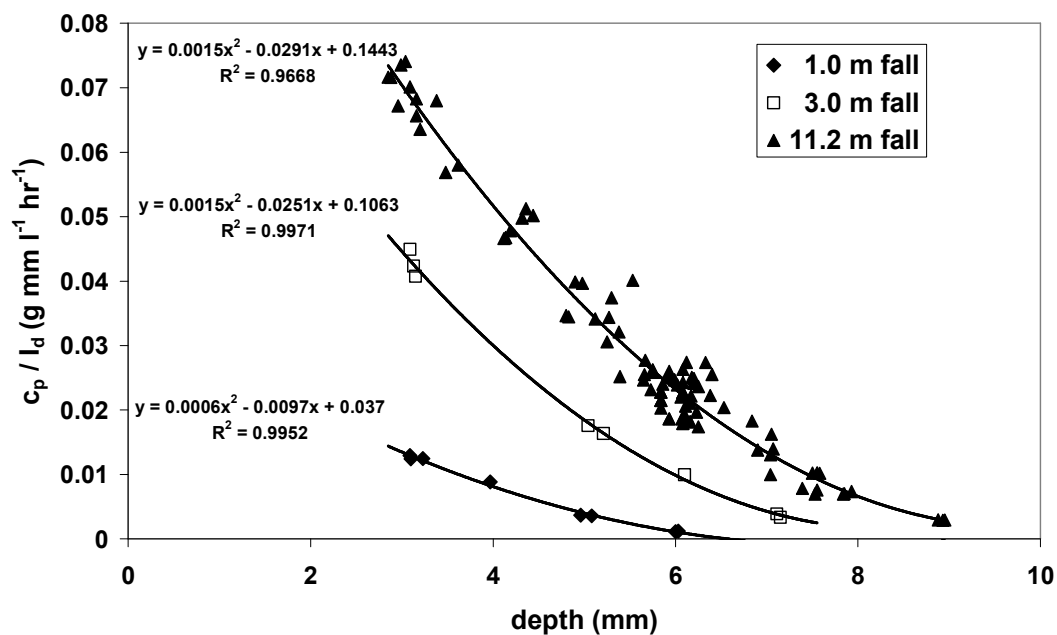


Figure 6. The effect of flow depth on sediment concentration per unit rainfall intensity for 0.2 mm sand under flows impacted by 2.7 mm drops falling from 1, 3 and 11.2 m (Kinnell, 2005a)

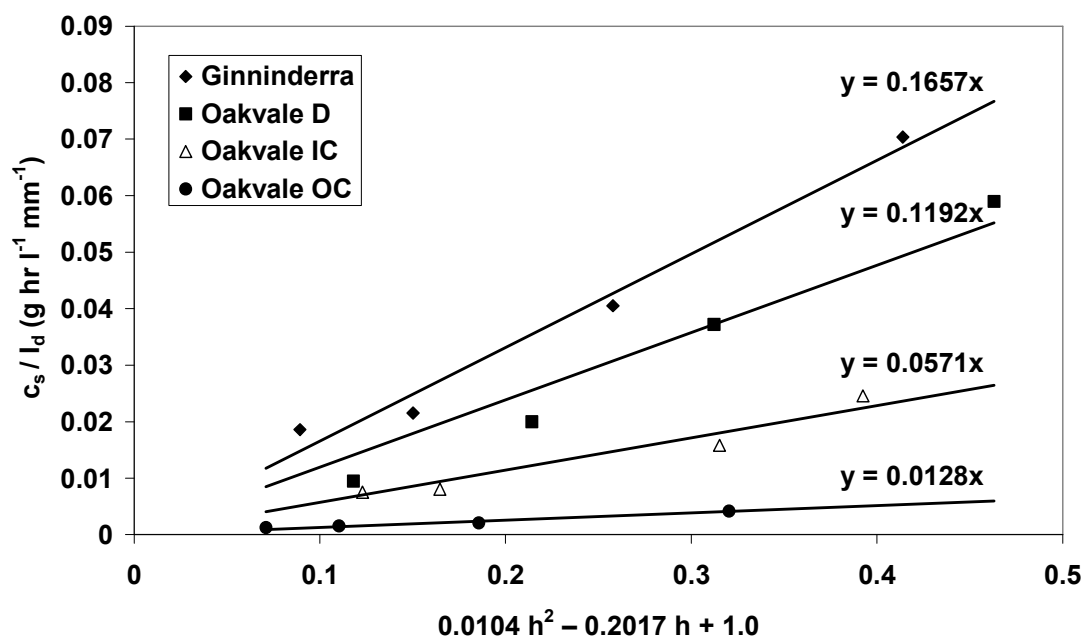


Figure 7. Relationships between $0.0104 h^2 - 0.2017 h + 1.0$ and sediment concentration per unit rainfall intensity for flows impacted by 2.7 mm drops travelling at near terminal velocity over soil monoliths (Kinnell, 2005b).

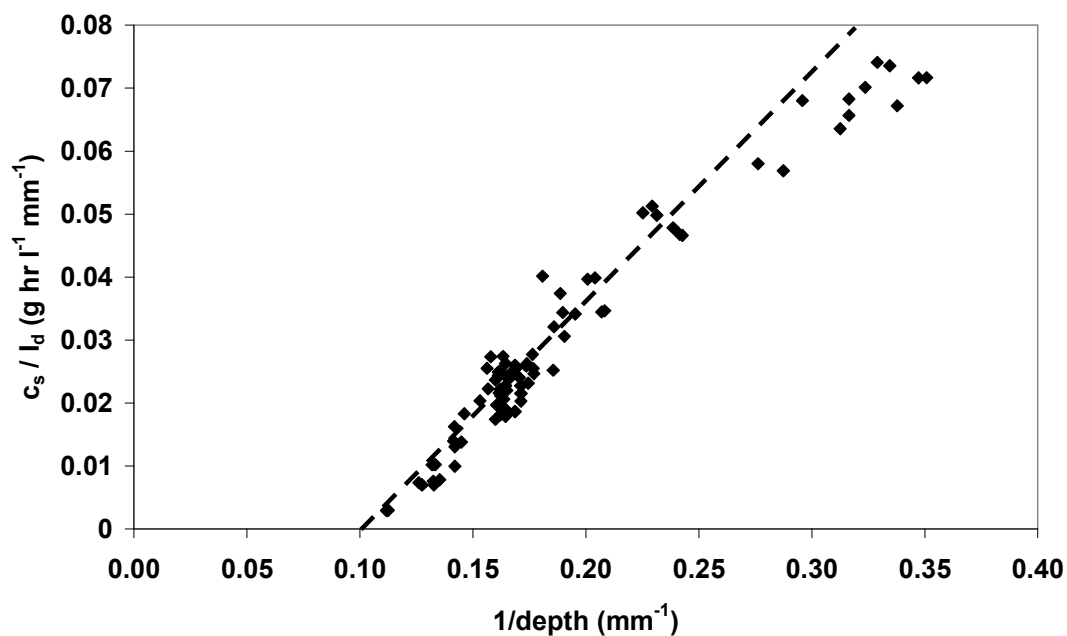


Figure 8. The relationship between sediment concentration per unit rainfall intensity and the inverse of flow depth for 2.7 mm drops travelling at close to terminal velocity impacting flows over 0.2 mm sand. The data are from the same experiments as used for Figure 4.

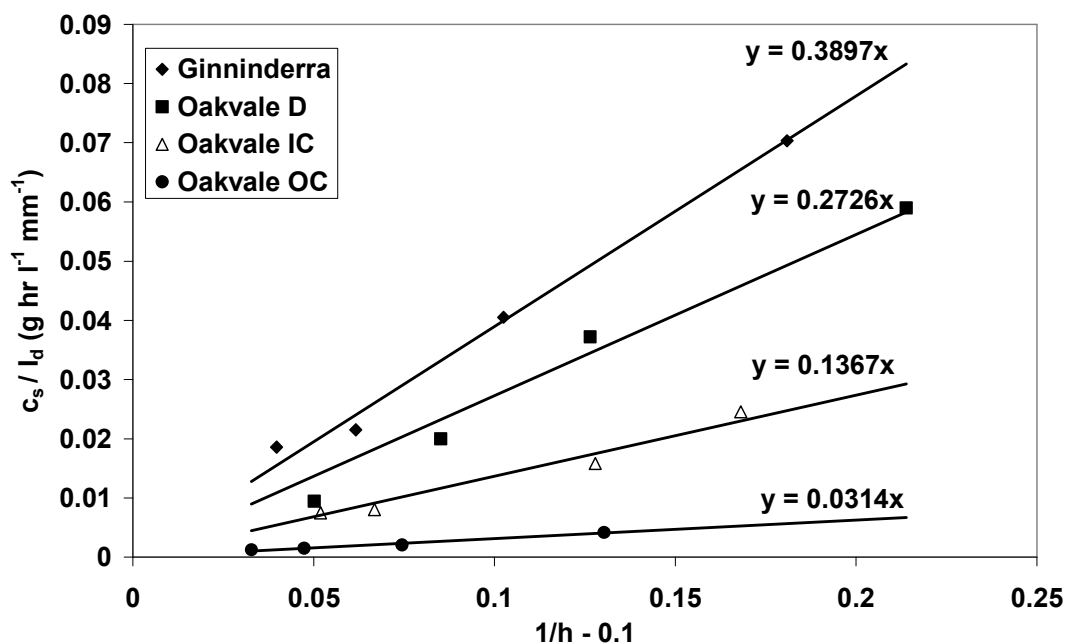


Figure 9. The relationship between sediment concentration per unit rainfall intensity and the inverse of flow depth minus 0.1 for 2.7 mm drops travelling at close to terminal velocity impacting flows over soil surfaces in the apparatus shown in Figure 1. The data are for the same experiments as used in Figure 7.